J|A|C|S
ARTICLES
Published on Web 12/20/2002

Ordered Mesoporous Silica with Large Cage-Like Pores: Structural Identification and Pore Connectivity Design by Controlling the Synthesis Temperature and Time

Jivaldo R. Matos,[†,⊥] Michal Kruk,[†] Lucildes P. Mercuri,[†,⊥] Mietek Jaroniec,*[,†] Lan Zhao,[‡,#] Tomoaki Kamiyama,[§] Osamu Terasaki,[‡] Thomas J. Pinnavaia,[∥] and Yu Liu[∥]

Department of Chemistry, Kent State University, Kent, Ohio 44242, Department of Physics, Tohoku University, Sendai 980-8578, Japan, Institute for Materials Research, Tohoku University, Sendai 980-8577, Japan, and Department of Chemistry and Center for Fundamental Materials Research, Michigan State University, East Lansing, Michigan 48824

Received August 29, 2002; E-mail: Jaroniec@columbo.kent.edu

Abstract: FDU-1 silicas with large cage-like pores (diameter about 10 nm) were synthesized under acidic conditions from tetraethyl orthosilicate in the presence of a poly(ethylene oxide)-poly(butylene oxide)-poly(ethylene oxide) triblock copolymer template B50−6600 ($EO_{39}BO_{47}EO_{39}$). High-resolution transmission electron microscopy and small-angle X-ray scattering provided strong evidence that FDU-1 silica synthesized under typical conditions is a face-centered cubic *Fm*3*m* structure with 3-dimensional hexagonal intergrowth and is not a body-centered cubic *Im*3*m* structure, as originally reported. Samples synthesized in a wide range of conditions (initial temperatures from 298 to 353 K; hydrothermal treatment at 333−393 K) exhibited similar XRD patterns and their nitrogen adsorption isotherms indicated a good-quality cage-like pore structure. The examination of low-pressure nitrogen adsorption isotherms for FDU-1 samples, whose pore entrance diameters were evaluated using an independent method, allowed us to conclude that low-pressure adsorption was appreciably stronger for samples with smaller pore entrance sizes. This prompted us to examine low-pressure adsorption isotherms for a wide range of samples and led us to a conclusion that the FDU-1 pore entrance size can be systematically enlarged from about 1.3 nm (perhaps even lower) to at least 2.4 nm without an appreciable loss of uniformity by increasing the temperature of the hydrothermal treatment or the initial synthesis. Further enlargement of pore entrance size was achieved for sufficiently long hydrothermal treatment times at temperatures of 373 K or higher, as seen from the shape of nitrogen desorption isotherms. This allowed us to obtain samples with uniform pore sizes, high adsorption capacity, and with pore entrances enlarged so much that their size was similar to the size of the pore itself, resulting in a highly open porous structure. However, in the latter case, there was evidence that the pore entrance size distribution was quite broad.

1. Introduction

The discovery of supramolecular-templated ordered mesoporous silicas (OMSs)[1−4] was a milestone in the synthesis of porous materials, providing an extension of ordered microporous structures of zeolites and zeotypes into the mesopore range (pore size 2−50 nm). Initially discovered OMSs, such as MCM-41,[1,2,5] MCM-48,[1,2,6] and FSM-16,[4] as well as many other important OMS,[7−12] such as SBA-3,[7] HMS,[8] KIT-1,[9] MSU-x,[11] and SBA-15[12] exhibit channel-like pore structures. These include a 2-dimensional (2-D) hexagonal (honeycomb) array of nonin-

[†] Department of Chemistry, Kent State University.
[‡] Department of Physics, Tohoku University.
[§] Institute for Materials Research, Tohoku University.
[∥] Department of Chemistry and Center for Fundamental Materials Research, Michigan State University.
[⊥] Permanent address: Instituto de Química da Universidade de São Paulo, C. P. 26.077, 05599-970, São Paulo, SP, Brazil.
[#] Permanent address: Department of Chemistry, Jilin University, Changchun, P. R. China.

(1) Kresge, C. T.; Leonowicz, M. E.; Roth, W. J.; Vartuli, J. C.; Beck, J. S. *Nature* **1992**, *359*, 710−712.
(2) Beck, J. S.; Vartuli, J. C.; Roth, W. J.; Leonowicz, M. E.; Kresge, C. T.; Schmitt, K. D.; Chu, C. T−W.; Olson, D. H.; Sheppard, E. W.; McCullen, S. B.; Higgins, J. B.; Schlenker, J. L. *J. Am. Chem. Soc.* **1992**, *114*, 10 834−10 843.
(3) Yanagisawa, T.; Shimizu, T.; Kuroda, K.; Kato, C. *Bull. Chem. Soc. Jpn.* **1990**, *63*, 988−992.
(4) Inagaki, S.; Fukushima, Y.; Kuroda, K. *J. Chem. Soc., Chem. Commun.* **1993**, 680−682.
(5) Chen, C.-Y.; Li, H.-X.; Davis, M. E. *Micropor. Mater.* **1993**, *2*, 17−26.
(6) Monnier, A.; Schuth, F.; Huo, Q.; Kumar, D.; Margolese, D.; Maxwell, R. S.; Stucky, G. D.; Krishnamurty, M.; Petroff, P.; Firouzi, A.; Janicke, M.; Chmelka, B. F. *Science* **1993**, *261*, 1299−1303.
(7) Huo, Q.; Margolese, D. I.; Ciesla, U.; Feng, P.; Gier, T. E.; Sieger, P.; Leon, R.; Petroff, P. M.; Schuth, F.; Stucky, G. D. *Nature* **1994**, *368*, 317−321.
(8) Tanev, P. T.; Pinnavaia, T. J. *Science* **1995**, *267*, 865−867.
(9) Ryoo, R.; Kim, J. M.; Ko, C. H.; Shin, C. H. *J. Phys. Chem. B* **1996**, *100*, 17 718−17 721.
(10) Attard, G. S.; Glyde, J. C.; Goltner, C. G. *Nature* **1995**, *378*, 366−368.
(11) Bagshaw, S. A.; Prouzet, E.; Pinnavaia, T. J. *Science* **1995**, *269*, 1242−1244.
(12) Zhao, D.; Huo, Q.; Feng, J.; Chmelka, B. F.; Stucky, G. D. *J. Am. Chem. Soc.* **1998**, *120*, 6024−6036.

10.1021/ja0283347 CCC: $25.00 © 2003 American Chemical Society

tersecting pores (e.g., the structure of MCM-41 and FSM-16) and 3-D cubic *Ia*3*d* structure with branched pore channels characteristic of MCM-48. The later discovery of ordered silicas with cage-like mesoporous structures (OSCMSs)[7,13] was a further major achievement in the synthesis of porous materials, extending the cage dimensions attainable for zeolites and zeotypes into the mesopore range. The amorphous character of pore walls of OSCMSs results in a lower degree of structural perfection and makes the structures less well-defined when compared to zeolites and zeotypes, but on the other hand, this character imposes less restrictions on the structure, which is expected to open wider opportunities in the tailoring of such properties as the pore size and pore connectivity. There are several well-documented and relatively well-defined structure types of OSCMSs, which include cubic *Pm*3*n* structure characteristic of both SBA-1[7,14] and SBA-6,[14] cubic *Im*3*m* structure of SBA-16,[12,14] and cubic *Fm*3*m* (cubic close-packed) structure of organic-modified SBA-12.[15] In addition, there is a range of OSCMSs that are mixtures of cubic close-packed and hexagonal close-packed ($P6_3/mmc$) structures with different contents of the two phases, different sizes of domains of pure phases, and so on.[15−17] SBA-2[13] and SBA-12[12] were found to belong to this group of mixed-phase materials with close-packed structures,[15−17] although they were initially identified as 3-D hexagonal ($P6_3/mmc$) materials.[12,13] The problems in SBA-2 and SBA-12 identification show that the structural assignment of a given OSCMS to a particular structural type is often difficult. This is because of the structural complexity of these materials, which in addition to sometimes limited size of their ordered domains and degree of structural perfection, causes that a substantial amount of information, such as transmission electron microscopy (TEM) images and electron diffraction (ED) patterns, X-ray diffraction (XRD) or small-angle X-ray scattering (SAXS) patterns, is required to complete the assignment. Other OSCMS structures were also reported,[12,18−21] some of which were poorly defined or weakly ordered, but they do not appear to be fully understood, and will require further studies.

There has been a long-standing interest in the synthesis of OSCMSs in the form of thin films,[22−25] fibers[26] and hierarchically ordered patterns,[27] because the 3-D pore structure of OSCMSs is expected to ensure the accessibility of the pores from the surface of the film, fiber, or pattern, which is often difficult to achieve in unidirectional pore systems. This beneficial property of OSCMS films has been taken advantage of in the development of a gas sensing system.[28] OSCMSs have recently attracted much interest as prospective catalysts, because their 3-D pore structures are expected to be less prone to blockage than channel-like structures. Therefore, the possibility of incorporation of catalytically active heteroatoms in silica frameworks of OSCMSs has been actively pursued.[29−36] The introduction of organic groups of catalytic or selective adsorption properties on the surfaces of OSCMSs is another new area of research.[37−39] Structures with cage-like pores are attractive as media for adsorption or immobilization of biomolecules,[40,41] such as enzymes. OSCMSs are also highly promising templates for the synthesis of quantum dots[42] and 3-D inverse replicas, including ordered mesoporous carbons,[43−45] and can be used to direct the growth of carbon nanotubes.[46]

Much work has recently been devoted to the development of methods to synthesize OSCMSs with tailored unit-cell dimensions, pore sizes, and pore connectivity.[31,47−58] In particular, the syntheses that use oligomer and block copolymer tem-

(13) Huo, Q.; Leon, R.; Petroff, P. M.; Stucky, G. D. *Science* **1995**, *268*, 1324−1327.
(14) Sakamoto, Y.; Kaneda, M.; Terasaki, O.; Zhao, D. Y.; Kim, J. M.; Stucky, G. D.; Shin, H. J.; Ryoo, R. *Nature* **2000**, *408*, 449−453.
(15) Sakamoto, Y.; Diaz, I.; Terasaki, O.; Zhao, D.; Perez-Pariente, J.; Kim, J. M.; Stucky, G. D. *J. Phys. Chem. B* **2002**, *106*, 3118−3123.
(16) Zhou, W.; Hunter, H. M. A.; Wright, P. A.; Ge, Q.; Thomas, J. M. *J. Phys. Chem. B* **1998**, *102*, 6933−6936.
(17) Hunter, H. M. A.; Garcia-Bennett, A. E.; Shannon, I. J.; Zhou, W.; Wright, P. A. *J. Mater. Chem.* **2002**, *12*, 20−23.
(18) Kramer, E.; Forster, S.; Goltner, C.; Antonietti, M. *Langmuir* **1998**, *14*, 2027−2031.
(19) Goltner, C. G.; Berton, B.; Kramer, E.; Antonietti, M. *Chem. Commun.* **1998**, 2287−2288.
(20) Zhang, W.; Glomski, B.; Pauly, T. R.; Pinnavaia, T. J. *Chem. Commun.* **1999**, 1803−1804.
(21) Kim, J. M.; Sakamoto, Y.; Hwang, Y. K.; Kwon, Y.-U.; Terasaki, O.; Park, S.-E.; Stucky, G. D. *J. Phys. Chem. B* **2002**, *106*, 2552−2558.
(22) Tolbert, S. H.; Schaffer, T. E.; Feng, J.; Hansma, P. K.; Stucky, G. D. *Chem. Mater.* **1997**, *9*, 1962−1967.
(23) Zhao, D.; Yang, P.; Margolese, D. I.; Chmelka, B. F.; Stucky, G. D. *Chem. Commun.* **1998**, 2499−2500.
(24) Lu, Y.; Ganguli, R.; Drewien, C. A.; Anderson, M. T.; Brinker, C. J.; Gong, W.; Guo, Y.; Soyez, H.; Dunn, B.; Huang, M. H.; Zink, J. I. *Nature* **1997**, *389*, 364−368.
(25) Zhao, D.; Yang, P.; Melosh, N.; Feng, J.; Chmelka, B. F.; Stucky, G. D. *Adv. Mater.* **1998**, *10*, 1380−1385.
(26) Yang, P.; Zhao, D.; Chmelka, B. F.; Stucky, G. D. *Chem. Mater.* **1998**, *10*, 2033−2036.
(27) Yang, P.; Deng, T.; Zhao, D.; Feng, P.; Pine, D.; Chmelka, B. F.; Whitesides, G. M.; Stucky, G. D. *Science* **1998**, *282*, 2244−2246.
(28) Yamada, T.; Zhou, H. S.; Uchida, H.; Tomita, M.; Ueno, Y.; Ichino, T.; Honma, I.; Asai, K.; Katsube, T. *Adv. Mater.* **2002**, *14*, 812−815.
(29) Ryoo, R.; Jun, S.; Kim, J. M.; Kim, M. J. *Chem. Commun.* **1997**, 2225−2226.
(30) Morey, M. S.; Davidson, A.; Stucky, G. D. *J. Porous Mater.* **1998**, *5*, 195−204.
(31) Hunter, H. M. A.; Wright, P. A. *Micropor. Mesopor. Mater.* **2001**, *43*, 361−373.
(32) Hartmann, M.; Vinu, A.; Elangovan, S. P.; Murugesan, V.; Bohlmann, W. *Chem. Commun.* **2002**, 1238−1239.
(33) Ikeue, K.; Nozaki, S.; Ogawa, M.; Anpo, M. *Catal. Lett.* **2002**, *80*, 111−114.
(34) Dai, L.-X.; Tabata, K.; Suzuki, E.; Tatsumi, T. *Chem. Mater.* **2001**, *13*, 208−212.
(35) Dai, L.-X.; Teng, Y.-H.; Tabata, K.; Suzuki, E.; Tatsumi, T. *Chem. Lett.* **2000**, 794−795.
(36) Vinu, A.; Dedecek, J.; Murugesan, V.; Hartmann, M. *Chem. Mater.* **2002**, *14*, 2433−2435.
(37) Diaz, I.; Mohino, F.; Perez-Pariente, J.; Sastre, E.; Wright, P. A.; Zhou, W. *Stud. Surf. Sci. Catal.* **2001**, *135* (on CD-ROM).
(38) Diaz, I.; Mohino, F.; Sastre, E.; Perez-Pariente, J. *Stud. Surf. Sci. Catal.* **2001**, *135* (on CD-ROM).
(39) Yoshitake, H.; Yokoi, T.; Tatsumi, T. *Chem. Lett.* **2002**, 586−587.
(40) Deere, J.; Magner, E.; Wall, J. G.; Hodnett, B. K. *Chem. Commun.* **2001**, 465−466.
(41) Han, Y.-J.; Watson, J. T.; Stucky, G. D.; Butler, A. *J. Mol. Catal. B: Enzymatic* **2002**, *17*, 1−8.
(42) Besson, S.; Gacoin, T.; Ricolleau, C.; Jacquiod, C.; Boilot, J.-P. *Nano Lett.* **2002**, *2*, 409−414.
(43) Ryoo, R.; Joo, S. H.; Kruk, M.; Jaroniec, M. *Adv. Mater.* **2001**, *13*, 677−681.
(44) Yu, C.; Stucky, G. D.; Zhao, D. In *Abstracts of 3rd International Mesostructured Materials Symposium*, July 8−11, 2002, PA-4, p 54.
(45) Zhao, D.; Yu, C.; Tian, B.; Fan, J.; Liu, X.; Yang, H.; Wang, L.; Shen, S.; Tu, B. In *Abstracts of 3rd International Mesostructured Materials Symposium*, July 8−11, 2002, KL-2, p 3.
(46) Zheng, G.; Zhu, H.; Luo, Q.; Zhou, Y.; Zhao, D. *Chem. Mater.* **2001**, *13*, 2240−2242.
(47) Kim, M. J.; Ryoo, R. *Chem. Mater.* **1999**, *11*, 487−491.
(48) Kim, J. M.; Stucky, G. D. *Chem. Commun.* **2000**, 1159−1160.
(49) Yamada, T.; Asai, K.; Ishigure, K.; Endo, A.; Zhou, H. S.; Honma, I. *Mater. Res. Soc. Symp. Proc.* **2000**, *628*, CC6.24.1−6.
(50) Kao, C.-P.; Lin, H.-P.; Chao, M.-C.; Sheu, H.-S.; Mou, C.-Y. *Stud. Surf. Sci. Catal.* **2001**, *135* (on CD-ROM).
(51) Yu, C.; Tian, B.; Fan, J.; Stucky, G. D.; Zhao, D. *J. Am. Chem. Soc.* **2002**, *124*, 4556−4557.
(52) Yu, C.; Yu, Y.; Zhao, D. *Chem. Commun.* **2000**, 575−576.
(53) Tattershall, C. E.; Jerome, N. P.; Budd, P. M. *J. Mater. Chem.* **2001**, *11*, 2979−2984.
(54) Matos, J. R.; Mercuri, L. P.; Kruk, M.; Jaroniec, M. *Langmuir* **2002**, *18*, 884−890.
(55) Kruk, M.; Antochshuk, V.; Matos, J. R.; Mercuri, L. P.; Jaroniec, M. *J. Am. Chem. Soc.* **2002**, *124*, 768−769.
(56) Van Der Voort, P.; Benjelloun, M.; Vansant, E. F. *J. Phys. Chem. B* **2002**, *106*, 9027−9032.

plates,[48−62] which are viable for a commercial production of OSCMSs, especially when cheap silica sources are used,[48,54] attracted a lot of interest. Block copolymer templates open an avenue for the synthesis of large-pore OSCMSs.[12,25,26,52,54,56,58] Oligomer and block copolymer templates are known from their ability to direct the formation of pores of appreciably different sizes depending on the temperature[12,50,54,63,64] and promising evidence for the temperature control of the pore entrance size was recently provided for copolymer templates.[55] Moreover, some copolymer-templated OSCMSs were found to lose the cage-like character of some of their pores during hydrothermal treatments,[54,57] especially at longer treatment times, leading to the development of more open pore structure, which was found to be beneficial from the point of view of the use of OSCMSs as templates and adsorption media.[45] The development of a more open structure may be similar to that reported recently for a polymeric-templated SBA-15 silica with 2-D hexagonally ordered structure of large mesopores connected via pores in the silica walls. These connecting pores were found to be markedly enlarged under high-temperature hydrothermal treatment conditions.[65]

Herein, results of the structure determination and an extensive exploration of the opportunities in the pore structure tailoring for a prominent member of OSCMS family are reported. The study was devoted to FDU-1 silica,[52,54,55,61,62] which is a highly ordered, large-pore OSCMS synthesized from TEOS in the presence of poly(ethylene oxide)-poly(butylene oxide)-poly(ethylene oxide) template. FDU-1 was reported to exhibit a large adsorption capacity,[52,54,62] a remarkable hydrothermal stability,[52,61] a uniform, narrowly defined pore entrance size,[55] and can be synthesized using a cost-efficient silica source.[54] The current work shows that FDU-1 is not a cubic *Im*3*m* structure, as reported earlier,[52,61] but a cubic *Fm*3*m* structure with 3-D hexagonal intergrowth, similar to SBA-12[15] and SBA-2.[16,17] It is demonstrated that the temperature and time control during the synthesis allows one to gradually change cage-like pores of FDU-1 to a highly open and accessible porous system with narrow pore size distribution. Evidence for the feasibility of tailoring the FDU-1 pore entrance size between 1.3 and at least 2.4 nm is also presented.

2. Experimental Section

Materials. The synthesis of FDU-1 silicas was carried out using the same synthesis gel composition as reported by Yu et al.:[52] 1 TEOS: 0.00735 B50−6600:6 HCl: 155 H_2O, where TEOS stands for tetraethyl orthosilicate and B50−6600 is a poly(ethylene oxide)-poly(butylene oxide)-poly(ethylene oxide) triblock copolymer ($EO_{39}BO_{47}EO_{39}$) from Dow Chemicals. A typical synthesis procedure was as follows.[54] 2 g of B50−6600 copolymer was dissolved in 120 g of 2 M HCl and stirred at room temperature until a homogeneous mixture was obtained. Subsequently, 8.32 g (8.92 mL) of TEOS was added and the resulting mixture was stirred vigorously in an open beaker for 1 day at room temperature. The precipitation was usually observed 30−40 min after the addition of TEOS. In several syntheses, the first step of the synthesis was carried out at a higher temperature (313−363 K), which in some cases required the mitigation of the loss of water, for instance by attaching a condenser to a flask in which the mixture was stirred. If needed, the mixture obtained after the first step of the synthesis was subjected to an additional hydrothermal treatment by transferring it to a Teflon-lined autoclave and heating at temperature in the range from 333 to 413 K for a period of time in the range from 3 h to 24 days without stirring. Finally, the precipitate was filtered out, washed with water, dried at 298 K, and calcined under nitrogen, which was then switched to air, at 813 K. Samples synthesized in a one-step procedure are denoted T*x*, where *x* is the synthesis temperature in degrees Kelvin, whereas samples synthesized in a two-step procedure are denoted T*x*H*y*-*t*, where *x* is the temperature of the first step, *y* is the temperature of the second step, *t* is the time of the second-step treatment in hours ("h") or days ("d"). When different samples synthesized under the same conditions are referred to, the number of the sample is appended to the end of the sample symbol. For instance, T298H373−6h2 denotes the second sample among samples synthesized at 298 K and hydrothermally treated at 373 K for 6 h.

Measurements. For TEM observations, the samples were studied using a JEM-3010 (Cs = 0.6 mm, resolution 0.17 nm) at 300 kV. High-resolution transmission electron microscopy (HRTEM) images and electron diffraction (ED) patterns were recorded with film (MEM) and a slow scan CCD (Gatan 794, 1k × 1k, pixel size 25 × 25 microns) using low-dose conditions. Films were scanned by AGFA Select Scan Plus. Small-angle powder X-ray scattering (SAXS) profiles were recorded on a homemade camera with imaging plate at transmission mode under vacuum. X-ray radiation was generated by Rigaku Rotating Anode (Cu K_α, 50 kV, 290 mA) with Graphite monochromator and the exposure time was 1 h.[66] Powder X-ray diffraction (XRD) patterns were recorded on a Rigaku Rotaflex diffractometer equipped with a rotating anode and Cu K_α radiation. Nitrogen adsorption measurements were carried out on a Micromeritics ASAP 2010 volumetric adsorption analyzer. Before the adsorption measurements, samples were outgassed at 473 K in the port of the adsorption analyzer.

Calculations. The BET specific surface area[67] was calculated from adsorption data in the relative pressure range from 0.04 to 0.2. The total pore volume[67] was estimated from the amount adsorbed at a relative pressure of 0.99. The micropore volume and the mesopore surface area were evaluated from a linear segment of the α_s plot[67,68] below the onset of the capillary condensation.[54] The external surface area and the sum of the micropore volume and the primary pore volume were evaluated from a linear segment of the α_s plot following the completion of the capillary condensation step.[54] The micropore volume estimated in the above way includes the contribution from the volume of the pores that connect the ordered cage-like mesopores, but this contribution is likely to be relatively small. The pore size distribution (PSD) was calculated by employing an algorithm based on the concept of Barrett, Joyner, and Halenda (BJH)[69] using a relation between the pore size and capillary condensation pressure for cylindrical pores derived on the basis of studies of the MCM-41 silicas with cylindrical pores.[70] The pore size is defined as a position of the maximum on PSD. Because of the fact that the geometry of primary mesopores of FDU-1

(57) Fan, J.; Yu, C.; Wang, L.; Sakamoto, Y.; Terasaki, O.; Tu, B.; Zhao, D. In *Abstracts of 3rd International Mesostructured Materials Symposium*, July 8−11, 2002, PA-22, p 72.
(58) Tattershall, C. E.; Aslam, S. J.; Budd, P. M. *J. Mater. Chem.* **2002**, *12*, 2286−2291.
(59) Kipkemboi, P.; Fogden, A.; Alfredsson, V.; Flodstrom, K. *Langmuir* **2001**, *17*, 5398−5402.
(60) El-Safty, S. A.; Evans, J. *J. Mater. Chem.* **2002**, *12*, 117−123.
(61) Yu, C.; Yu, Y.; Miao, L.; Zhao, D. *Micropor. Mesopor. Mater.* **2001**, *44*−*45*, 65−72.
(62) Tian, B.; Liu, X.; Yu, C.; Gao, F.; Luo, Q.; Xie, S.; Tu, B.; Zhao, D. *Chem. Commun.* **2002**, 1186−1187.
(63) Prouzet, E.; Pinnavaia, T. J. *Angew. Chem., Int. Ed. Engl.* **1997**, *36*, 516−518.
(64) Kruk, M.; Jaroniec, M.; Ko, C. H.; Ryoo, R. *Chem. Mater.* **2000**, *12*, 1961−1968.
(65) Fan, J.; Yu, C.; Wang, L.; Tu, B.; Zhao, D.; Sakamoto, Y.; Terasaki, O. *J. Am. Chem. Soc.* **2001**, *123*, 12 113−12 114.
(66) Kamiyama, T.; Kimura, H. M.; Sasamori, K.; Inoue, A. *Scr. Metall.* **2001**, 1297−1301.
(67) Sing, K. S. W.; Everett, D. H.; Haul, R. A. W.; Moscou, L.; Pierotti, R. A.; Rouquerol, J.; Siemieniewska, T. *Pure Appl. Chem.* **1985**, *57*, 603−619.
(68) Jaroniec, M.; Kruk, M.; Olivier, J. P. *Langmuir* **1999**, *15*, 5410−5413.
(69) Barrett, E. P.; Joyner, L. G.; Halenda, P. P. *J. Am. Chem. Soc.* **1951**, *73*, 373−380.
(70) Kruk, M.; Jaroniec, M.; Sayari, A. *Langmuir* **1997**, *13*, 6267−6273.

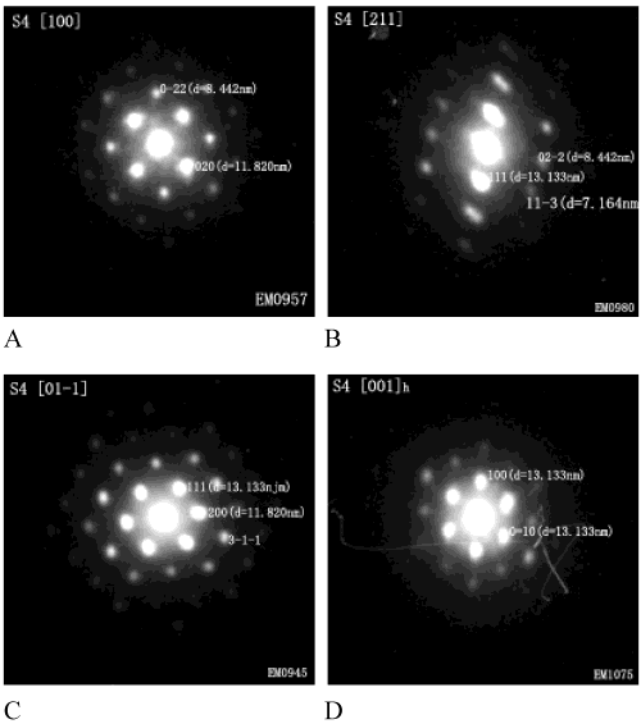

Figure 1. Electron diffraction patterns of FDU-1 (sample T298H373−6h2).

can be approximated by a sphere rather than a cylinder, this method is likely to lead to a systematic underestimation of the diameter of cage-like pores by about 2 nm, as discussed in more detail later. The primary mesopore cage diameter, w_d, of FDU-1 was also evaluated using the following equation for a cubic structure with spherical cavities[71]

$$w_d = a\left(\frac{6}{\pi\nu}\frac{V_p\rho}{1 + V_p\rho + V_{mi}\rho}\right)^{1/3} \quad (1)$$

where a is the unit-cell parameter, ν is the number of cavities in the unit cell ($\nu = 4$ for face-centered cubic structure), V_p is the primary mesopore volume, and V_{mi} is the volume of the pores in the walls of the primary mesopores.

3. Results and Discussion

TEM. A calcined sample T298H373−6h2 synthesized at room temperature and subjected to the hydrothermal treatment at 373 K (typical FDU-1 synthesis), and a calcined sample T303 synthesized at room temperature were extensively studied using HRTEM to determine the ordered structure type for the FDU-1 silicas. These two samples were shown earlier to exhibit a uniform pore entrance diameter, which was in the mesopore range (above 2 nm) for T298H373−6h2, and in the micropore range (below 2 nm) for T303.[55] The results for T298H373−6h2 are briefly described below, whereas the results for T303 are provided as Supporting Information. T298H373−6h2 belongs to the crystal system of either cubic or tetragonal symmetry, because its electron diffraction (ED) pattern (Figure 1A) showed a 4-fold axis of symmetry. 3-fold symmetry was also confirmed from Fourier transform of HRTEM image. If both of these symmetry elements correspond to the same structure, the structure is cubic. Both ED and SAXS (see below) patterns can be indexed on a cubic lattice of face-centered cubic

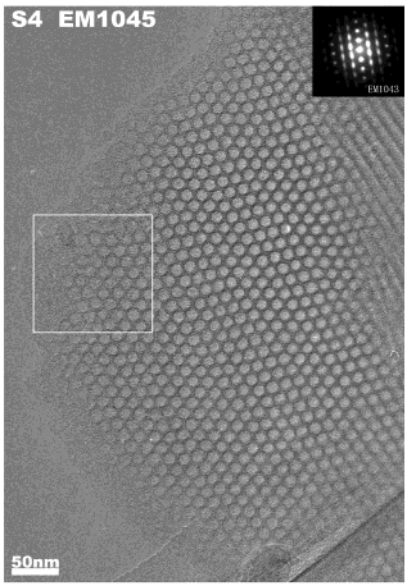

Figure 2. Transmission electron microscopy image of FDU-1 (sample T298H373−6h2).

type (F-type) and the results are given in Supplementary Tables 1S and 2S. The unit-cell parameters determined from ED patterns and SAXS pattern were 23.6 and 21.6 nm, respectively. Taking into account errors related to the camera length, which is not precise, the difference between unit cell parameters obtained from SAXS and ED is acceptable. Some ED patterns for T298H373−6h2 clearly showed strong diffuse streaks (see inset in Figure 2). The diffuse streaks are likely to arise from the presence of an intergrowth of hexagonal close packed (hcp) and cubic close packed (ccp) phases.[15] This identification was confirmed by examining the corresponding HR TEM image (Figure 2), which revealed narrow bands of cubic F-type structures that are in twin relation with each other, similar to those observed in SBA-12 silica[15] and discussed elsewhere.[15,72,73] It should be noted that SBA-12 exhibited a poorly resolved XRD pattern with a single well-pronounced peak,[15] whereas FDU-1 exhibited SAXS and XRD patterns with multiple peaks (see below). ED patterns shown in Figure 1, parts A, B, and C, were identified, respectively, as ED patterns of [100], [211], and [01−1] incidence of a cubic phase, with a lattice constant (unit-cell parameter) of 23.6 nm. ED pattern shown in Figure 1D cannot be indexed as an ED pattern for a cubic phase. If Figure 1D is regarded as an ED pattern for [001] incidence of a hexagonal phase, the resulting lattice constant, a_h, for such a hexagonal phase is 16.7 nm, which is consistent with the relationship in the intergrowth of hcp and ccp structures: $a_c = 1.414\ a_h$.[15] This provides a strong evidence for the presence of an intergrowth of hcp and ccp structures in the FDU-1 T298H373−6h2 sample. Figure 1A is an ED pattern of [100] incidence of a cubic phase and the corresponding HRTEM image is shown in Supporting Figure 1AS. Figure 1B is an ED pattern of [211] incidence of a cubic phase and the corresponding HREM image is shown in Supporting Figure 1BS. Figure 1C is an ED pattern of [01−1] incidence of a cubic phase and the corresponding HREM image is shown in Supporting Figure 1CS. Figure 1D is an ED pattern

(71) Ravikovitch, P. I.; Neimark, A. V. *Langmuir* **2002**, *18*, 1550−1560.

(72) Terasaki, O.; Ohsuna, T.; Alfredsson, V.; Bovin, J.-O.; Watanabe, D.; Carr, S. W.; Anderson, M. W. *Chem. Mater.* **1993**, *5*, 452−458.

(73) Ohsuna, T.; Terasaki, O.; Alfredsson, V.; Bovin, J.-O.; Watanabe, D.; Carr, S. W.; Anderson, M. W. *Proc. R. Soc. London A* **1996**, *452*, 715−740.

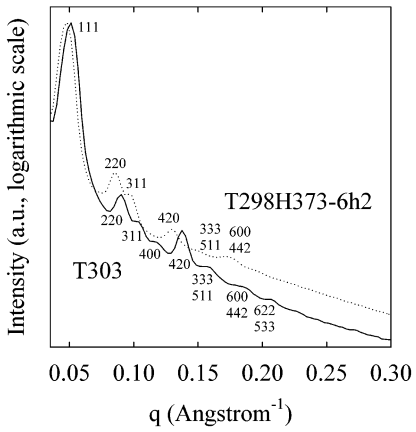

Figure 3. Small-angle X-ray scattering patterns for FDU-1 silica samples T303 and T298H373−6h2.

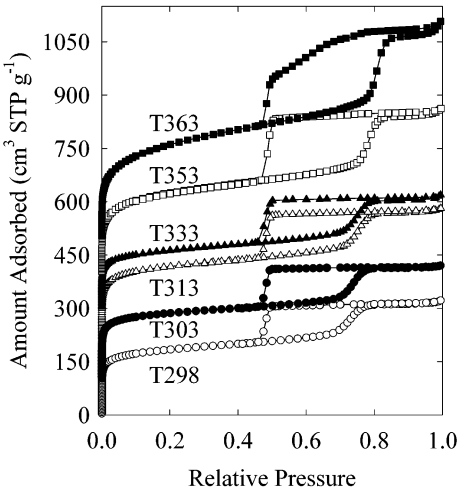

Figure 4. Nitrogen adsorption isotherms for FDU-1 samples synthesized at different temperatures. Data for T298, T313, and T333 are taken from ref 44. Data for T303 are taken from ref 55. The isotherms for T303, T313, T333, T353, and T363 samples were offset vertically by 100, 200, 300, 400, and 500 cm^3 STP g^{-1}, respectively.

of [001] incidence of the 3-D hexagonal phase and the corresponding HREM image is shown in Supporting Figure 1DS. Reflections that can be indexed as 111, 200, 220, 311, 222, 420, 333, 422, and 440 are observed in ED patterns. Observed conditions: {*hkl*: *h*+*k*, *k*+*l*, *l*+*h* even}, {*0kl*: *k*, l even}, {*hhl:* *h*+*l* even}, {*00l*: l even} suggest that *F*43*m*, *F*432, *Fm*3, *F*23 and *Fm*3*m* are possible space groups. *Fm*3*m* is chosen as the highest space group for T298H373−6h2. The FDU-1 structure determined above is similar to that of organic-modified SBA-12 silica[15] and consequently, it is expected that each mesopore in FDU-1 structure (except for the pores adjacent to the surface of FDU-1 particles) is connected with its twelve nearest-neighbor mesopores, as in the structure of organic-modified SBA-12.[15] TEM images and ED patterns recorded for T303 sample synthesized without a hydrothermal treatment were generally similar to those for the T298H373−6h2 sample, and it was clear that this sample was also a face-centered cubic material, which appeared to contain 3-D hexagonal intergrowth (see Supporting Information).

SAXS. SAXS patterns for calcined T303 and T298H373−6h2 samples are shown in Figure 3, whereas the peak positions, peak assignment and the corresponding lattice parameters are provided in Supplementary Tables 2S and 4S. The SAXS pattern for the T303 FDU-1 sample featured at least eight reflections that can be indexed as 111, 220, 311, 400, 420, (333, 511), (600, 442), and (622, 533) reflections of a face-centered cubic phase. The SAXS pattern recorded for the T298H373−6h2 FDU-1 silica was very similar to that for T303, but in the former case, the reflections were shifted to lower angles, which indicate larger unit-cell dimensions, and were somewhat less resolved. Nonetheless, reflections that can be indexed as 111, 220, 311, 420 and (600, 442) peaks, were clearly seen. The SAXS patterns for these two samples were quite similar to powder XRD patterns reported earlier for the FAU zeolite structure of face-centered cubic symmetry.[73] The estimation of the unit-cell size on the basis of positions of particular reflections was quite consistent (see Supporting Tables 2S and 4S, and Supporting Figure 4S), especially when one takes into account the presence of stacking faults and 3-D hexagonal intergrowth, as revealed by HR TEM and ED studies. It should be noted that in the case of the *Fm*3*m* cubic structure, which was determined for T298H373−6h2 sample on the basis of its TEM images and ED patterns, the occurrence of (200) reflection is expected. However, the (200) reflection would be located close to the most prominent (111) reflection and might not be strong enough to emerge as a separate peak, especially as the intensity of the background appears to be high for low *q* values.

XRD. Powder XRD patterns for calcined FDU-1 samples prepared in a wide range of conditions were generally very similar to one another (see Supporting Figure 5S) and to the SAXS patterns, the latter being better resolved (see Figure 3). In the case of some samples with larger unit-cell dimensions, main (111) peaks appeared to be located at angles below the lower angular limit of the powder X-ray diffractometer used, and thus were not recorded. Nonetheless, the XRD patterns shown in Supporting Figure 5S clearly indicate that very similarly structured materials formed in a wide range of conditions, including the initial synthesis temperature from room temperature to 363 K, and the second-step synthesis temperatures in the range from 333 to 413 K. The above findings corroborate earlier findings that FDU-1 forms in the temperature range from 273 to 333 K,[52] but extend the upper limit of this range to about 363 K. On the basis of the XRD and SAXS data, the unit-cell parameter for the calcined FDU-1 samples tended to increase as the synthesis temperature was increased. A similar trend was reported earlier for the SBA-16 silica with cage-like mesopores.[50]

Nitrogen Adsorption. Samples Prepared in One-Step Synthesis. Nitrogen adsorption isotherms for silica samples synthesized at different temperatures in a one-step procedure are shown in Figure 4. With an exception for T363, the isotherms were characteristic of materials with large, uniform, cage-like mesopores,[25,26,53,54] that is, mesopores with entrances much narrower than the pore interiors,[54,55,71,74,75] because the capillary evaporation (at a relative pressure of 0.45−0.5) was significantly delayed with respect to the capillary condensation. This gave rise to a broad hysteresis loop.[67,71,75] If the pore structure is more open, for instance channel-like (with no constrictions), then hysteresis loops are also observed above the lower pressure limit of adsorption−desorption hysteresis

(74) Mason, G. *J. Colloid Interface Sci.* **1992**, *88*, 36−46.
(75) Kruk, M.; Jaroniec, M. *Chem. Mater.* **2001**, *13*, 3169−3183.

Table 1. Structural Properties of the Samples Synthesized in a One-Step Procedure[a]

sample	S_{BET} ($m^2\ g^{-1}$)	V_t ($cm^3\ g^{-1}$)	w (nm)	V_p ($cm^3\ g^{-1}$)	S_{ex} ($m^2\ g^{-1}$)	V_{mi} ($cm^3\ g^{-1}$)	S_p ($m^2\ g^{-1}$)
T298[b]	640	0.49	8.7[d]	0.27	20	0.20	190
T303[c]	650	0.49	9.0[d](10.6)[e]	0.26	10	0.21	170
T313[b]	760	0.59	9.5[d](11.2)[f]	0.31	20	0.24	220
T333[b]	570	0.49	9.3[d](11.1)[f]	0.29	20	0.16	200
T353	800	0.71	10.5[d](12.1)[f]	0.42	30	0.23	270
T363	940	0.92	11.6[d]	0.57	50	0.25	440

[a] S_{BET}, BET specific surface area; V_t, total pore volume; w, primary mesopore diameter; V_p, primary mesopore volume; S_{ex}, external surface area; V_{mi}, micropore volume (including the volume of the connecting pores, if the latter are of diameter below about 4 nm); S_p, primary mesopore surface area. [b] The data were reported in ref 54. [c] Pore entrance size of this sample was determined in ref 54. [d] Pore cage diameter was estimated using a method developed for cylindrical rather than spherical pores. [e] Pore cage diameter calculated using eq 1 from the unit-cell parameter determined on the basis of SAXS data. [f] Pore cage diameter calculated using eq 1 from the unit-cell parameter determined on the basis of XRD data.

(relative pressure of 0.4−0.5 for nitrogen at 77 K), but are usually narrow.[67,70] The prominent delay in the capillary evaporation observed for cage-like pores is related to the lack of direct access of the adsorbate (gas) condensed in the pore interiors to the surrounding gas phase, because of the presence of the adsorbate condensed in the narrower connecting pores.[71,74−77] It is known that the capillary evaporation from the interior of a cage-like pore takes place either at pressure at which the capillary evaporation from any of the connecting pores takes place, or at the lower limit of adsorption−desorption hysteresis, whichever of these pressure values is higher.[54,75] This leads to the occurrence of broad hysteresis loops for cage-like pores that are large enough to exhibit capillary condensation at pressures significantly higher than the lower limit of adsorption−desorption hysteresis and are connected with the surrounding with constrictions that exhibit capillary evaporation below this limit.

The behavior observed for the T298−T353 samples corresponds to the above description, which provides evidence that the pores are cage-like and the pore entrance size is relatively small. On the basis of earlier studies of adsorption and desorption from cylindrical pores,[70,78] one can conclude that when the nitrogen capillary evaporation at 77 K from a cage-like pore is delayed to the lower pressure limit of hysteresis, the pore entrance diameter has to be below about 5 nm. This is because the connecting pores of size above 5 nm would exhibit capillary evaporation above this pressure limit, with concomitant capillary evaporation from the interiors of the cage-like pores. T363 sample exhibited adsorption properties different from those of the T298−T353 samples, because the capillary evaporation for the former sample began at relative pressures much higher than the lower limit of adsorption−desorption hysteresis (see Figure 4). On the basis of the discussion presented above, this earlier onset of the capillary evaporation can be attributed to the existence of percolation pathways[77] consistent of pore entrances of sizes larger than about 5 nm, which would provide a direct access of the adsorbate condensed in the interiors of cage-like pores to the surrounding gas phase. This would lead to the capillary evaporation from mesopores above the lower pressure limit of hysteresis. The broadness of the relative pressure range at which the capillary evaporation took place for T363 (from about 0.75 to 0.45) suggests a broad distribution of pore entrance sizes. Capillary evaporation from some mesopores of the T363 sample took place at the lower limit of hysteresis (0.45−0.5), which provides evidence that this sample also exhibits an appreciable fraction of pore entrances of size below 5 nm. The broad distribution of the pore entrance sizes was not expected from the XRD pattern for T363 (Supporting Figure 5DS), which was similar to the XRD patterns for the T298−T353 samples synthesized at lower temperature (see Supporting Figure 5AS). It can be concluded that the one-step synthesis allows one to obtain ordered silicas with cage-like pores when the synthesis temperature is not higher than 353 K, whereas a more open porous structure is formed at 363 K. It should be noted that argon adsorption studies,[79,80] which will be reported elsewhere,[81] indicated that the T353 sample exhibited a small fraction of pore entrances of diameter above about 4 nm, whereas the samples synthesized at lower temperatures (298−333 K) did not exhibit pore entrances of size above 4 nm.

As can be seen in Table 1, an increase in temperature in the one-step synthesis generally resulted in an increase in the BET specific surface area, pore cage diameter (see PSDs in Supporting Figure 6S), and total pore volume. This is in contrast to the behavior recently reported for SBA-16,[56] for which a decrease in the total pore volume and relatively constant mesopore cage diameter was observed as the temperature of the one-step synthesis increased. All samples from the one-step synthesis were microporous to a significant extent, as inferred from the α_s plot analysis (see an illustrative α_s plot for T303 in Supporting Figure 7S). The micropore surface area and micropore volume constituted a significant fraction of the total pore volume and specific surface area. For samples synthesized at lower temperatures, the micropore volume was only slightly lower than the primary mesopore volume.[54] As was discussed elsewhere, the occurrence of microporosity of FDU-1[54] and other copolymer-templated silicas[64,82] is a result of the occlusion of the poly(ethylene oxide) chains (EO_n) of the copolymer template in the walls of the as-synthesized ordered silica. The micropores in the template-free silicas can be identified as voids in the silica framework where the EO_n chains of the template were located.[64,82] Obviously, the size and volume of these voids may change upon the template removal, and some may even become inaccessible. For some FDU-1 samples, the pores that connect the large cage-like mesopores may also be in the micropore

(76) Ball, P. C.; Evans, R. *Langmuir* **1989**, *5*, 714−723.
(77) Liu, H.; Zhang, L.; Seaton, N. A. *J. Colloid Interface Sci.* **1993**, *156*, 285−293.
(78) Kruk, M.; Jaroniec, M.; Sakamoto, Y.; Terasaki, O.; Ryoo, R.; Ko, C. H. *J. Phys. Chem. B* **2000**, *104*, 292−301.
(79) Jaroniec, M. In *Abstracts of 3rd International Mesostructured Materials Symposium*, July 8−11, 2002, KL-14, p 36.
(80) Jaroniec, M.; Kruk, M. In *Abstracts of 3rd International Mesostructured Materials Symposium*, July 8−11, 2002, PB-12, p 130.
(81) Kruk, M.; Jaroniec, M. *Chem. Mater.*, submitted.
(82) Ryoo, R.; Ko, C. H.; Kruk, M.; Antochshuk, V.; Jaroniec, M. *J. Phys. Chem. B* **2000**, *104*, 11 465−11 471.

Table 2. Structural Properties of the Samples Synthesized in a Two-Step Procedure with the First Step at Room Temperature[a]

sample	S_{BET} ($m^2\ g^{-1}$)	V_t ($cm^3\ g^{-1}$)	w (nm)	V_p ($cm^3\ g^{-1}$)	S_{ex} ($m^2\ g^{-1}$)	V_{mi} ($cm^3\ g^{-1}$)	S_p ($m^2\ g^{-1}$)
T298H373−6h1[b]	930	0.78	10.6[d]	0.46	30	0.27	300
T298H373−6h2[c]	820	0.68	10.6[d](12.0)[e]	0.39	20	0.25	240
T298H373−12h	820	0.72	10.8[d]	0.44	20	0.25	260
T298H373−1d1[b]	880	0.90	11.4[d]	0.65	30	0.20	430
T298H373−1d2	770	0.73	11.3[d]	0.48	20	0.20	300
T298H373−4d	720	0.85	12.2[d]	0.71	30	0.12	440
T298H373−12d	610	0.90	13.4[d]	0.77	30	0.09	390
T298H373−24d	610	0.98	13.7[d]	0.85	40	0.07	420

[a] See Table 1.

size range, as shown elsewhere[55] and will be further discussed below. Except for the T363 sample that was found to exhibit highly nonuniform pore window size, the primary (ordered) mesopore surface area constituted only about 25−35% of the specific surface area for the FDU-1 samples from the one-step synthesis, whereas the primary mesopore volume did not exceed 0.42 $cm^3\ g^{-1}$.

Samples Prepared in a Two-Step Synthesis. A typical way to increase the mesopore volume and the pore size of polymer-templated silicas is to subject them to a hydrothermal treatment at higher temperature.[12,50,54,56,64] The evolution of nitrogen adsorption isotherms for samples synthesized at room temperature and hydrothermally treated at 373 K can be seen in Figure 5, whereas the corresponding structural parameters are listed in Table 2. The hydrothermal treatment for as short as 6 h already led to an appreciable increase in the specific surface area, pore volume, and pore cage diameter with the retention of a cage-like nature of the mesopores, as seen from the shape of the adsorption−desorption hysteresis loop.[54] As reported elsewhere, the discussed hydrothermal treatment conditions (373 K, 6 h) led to a marked enlargement of the pore entrance diameter, which was found to be about 2.4 nm for the T298H373−6h2 sample, and was almost twice as large as that of the T303 sample synthesized at room temperature (about 1.3 nm).[55] For both T303 and T298H373−6h2, there was evidence that the pore entrance size was relatively uniform.[55] As the time of the hydrothermal treatment at 373 K was increased, the same shape of the adsorption isotherm was observed for the first 12 to 24 h (see Figure 5), whereas for longer times, the onset of capillary evaporation shifted from the lower limit of hysteresis to higher pressures. This indicates the development of a more open pore structure. The shape of the isotherm for a sample obtained after 4 d of the treatment still suggested the retention of an appreciable fraction of cage-like pores, although there was clear evidence for the formation of pore entrances of diameter 5 nm or larger. We have already reported similar, although less extensive, changes in adsorption isotherms for the FDU-1 samples synthesized using sodium silicate or TEOS as a silica source and hydrothermally treated for periods of 1 day or less.[54] Longer treatment times (12 and 24 d) resulted in an almost complete loss of a cage-like character of the porosity. For these samples, upper parts of the hysteresis loops were as narrow as those for channel-like pores or other open pore systems, but there was also some broadening and tailing of the hysteresis loops, which indicates the presence of some constrictions in the porous structure. In principle, in the case of the FDU-1 silica, the open pore structure may develop as a result of (i) the enlargement of the pore entrance size with retention of the original pore structure, (ii) the fusion of adjacent pore entrances, (iii) the development of large holes in the pore walls, and (iv) the transformation to a different structure. As far as the enlargement of the pore entrance size with retention of the original structure is concerned, some limitations on the maximum pore entrance size are expected because of the pore structure geometry. In particular, if each pore in the close-packed structure of FDU-1 is connected to all of its twelve neighbors and the diameters of all these connections are the same, the diameter of each pore entrance should not exceed the radius of the cage-like pore, otherwise the connections would coalesce. The pore radius for the FDU-1 samples studied herein was about 5−7 nm (see Tables 1, 2 and Supporting Table 5S), so the structures as open as those for samples hydrothermally treated for 4−24 days at 373 K are not likely to develop merely through the enlargement of the existing pore entrances. Therefore, the coalescence of adjacent pore entrances and the development of large holes in pore walls, as reported for SBA-15 heated at 403 K,[65] are both likely to contribute to the development of a more open pore structure for longer hydrothermal treatment times. As far as the possibility of phase transformation is concerned, the examination of the XRD patterns (Supporting Figure 5CS and 5DS) suggests the lack of any prominent phase transformation, although it appears that additional single peaks developed for some samples between the 111 and 220 reflections of the cubic F-type structure. This additional reflection may possibly be identified as the (102) reflection of the 3-D hexagonal

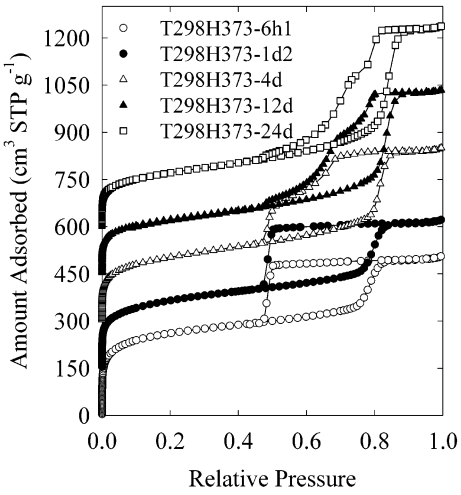

Figure 5. Nitrogen adsorption isotherms for FDU-1 samples synthesized at room temperature and hydrothermally treated for different periods of time ranging from 6 h to 24 days. Data for T298H373−6h1 are taken from ref 54. The isotherms for T298H373−1d2, −4d, −12d, and −24d samples were offset vertically by 150, 300, 450, and 600 cm^3 STP g^{-1}, respectively.

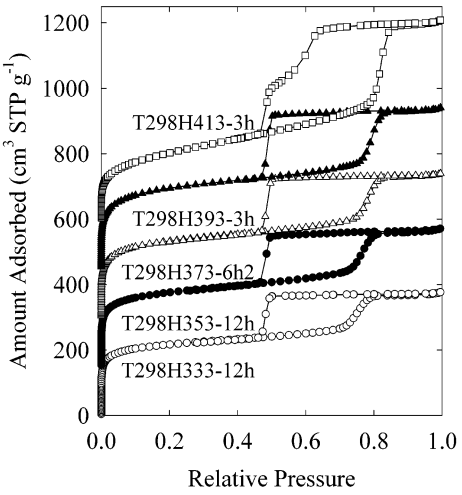

Figure 6. Nitrogen adsorption isotherms for FDU-1 samples synthesized at room temperature and hydrothermally treated at different temperatures ranging from 333 to 413 K. Data for T298H373−6h2 are taken from ref 55. The isotherms for T298H353−12h, −373−6h2, −393−3h, and −413−3h samples were offset vertically by 150, 300, 450, and 600 cm^3 STP g^{-1}, respectively.

intergrowth. These XRD data suggest us that the enlargement of pore entrances in the FDU-1 structure is likely to involve no phase transformation, despite the fact that phase transformations involving OSCMSs are feasible.[83] It should be noted that Zhao et al. recently presented results that suggest the retention of the pore structure symmetry, as seen from XRD and TEM, during the development of open pore structure of the SBA-16 silica (typically with cage-like pores) at temperatures of 373−413 K.[57] Zhao et al. also used a hydrothermal treatment at 403 K to enlarge the pore entrance size of FDU-1, to make it more suitable as a template for the synthesis of an ordered mesoporous carbon replica.[45,57]

As seen in Table 1, the hydrothermal treatment allowed us to obtain the FDU-1 samples not only with a good reproducibility of the pore diameter, but also with reasonable reproducibility of other structural parameters, such as the pore volume and specific surface area. Longer treatment times led to a reduction of the specific surface area and micropore volume, with a concomitant increase in the total pore volume, primary mesopore volume, area and diameter (for the latter, see also PSDs in Supporting Figure 8S).

The onset of the transition from a cage-like to a more open porous structure depends on the temperature of the hydrothermal treatment. Nitrogen adsorption isotherms for the FDU-1 samples hydrothermally treated at 333 and 353 K provide evidence of the lack of development of a more open porous structure even after 48 and 24 h, respectively. On the other hand, the development of pore entrances above 5 nm was already apparent after 6 h of treatment at 393 K (see Supporting Figure 9S), although there was no evidence for it after 3 h (see Figure 6). The hydrothermal treatment at 413 K for 3 h was sufficient to develop a more open pore structure (Figure 6), which appears to be similar to that obtained after hydrothermal treatment at 393 K for 12 h and at 373 K for 4 d. A very open porous structure was obtained after heating at 413 K for as short as 12 h (Supporting Figure 9S), whereas a similar porous structure was found to develop after 12−24 days of heating at 373 K (Figure 5). Interestingly, the materials with both cage-like pores and open pore structures were found to exhibit relatively narrow PSDs (see Supporting Figures 8S, 10S, and 11S), so the pore entrance enlargement appeared to be accompanied by neither the decrease of the pore diameter uniformity, nor the loss of the pore structure symmetry. When compared with the samples with uniform cage-like pores, the materials with more open structures usually exhibited larger total pore volumes and primary mesopore volumes, and lower specific surface areas and micropore volumes (see α_s plot for the T298H373−24d sample in Supporting Figure 7S).

As can be seen in Figure 6 and Supporting Table 5S, an increase in temperature of the second-step hydrothermal treatment from 333 to 393 K can be used to systematically increase the adsorption capacity, primary mesopore volume (up to 0.46 cm^3 g^{-1}) and the pore diameter of the FDU-1 silica (see PSDs in Supporting Figure 10S). The samples synthesized in the two-step procedure exhibited appreciable microporosity (see α_s plot for T298H373−6h2 in Supporting Figure 7S) and the primary mesopore area constituted significantly less than half of the specific surface area (see Table 2 and Supporting Table 5S). The external surface area of all samples studied herein was low. If one wants to obtain a material with large cage-like pores, the treatment time needs to be controlled to avoid the loss of cage-like character of the pore structure, which was discussed above. On the other hand, if the development of a highly open, ordered pore structure with narrow PSD is intended, extended treatment times at higher temperatures should be used. It is also possible to synthesize FDU-1 above room temperature and subject it to a further hydrothermal treatment at higher temperatures (see data in Supporting Table 5S). However, no apparent benefits of this more complicated synthesis procedure were found, when carefully compared to the results of the two-step synthesis with initial step at room temperature.

It should be noted that the PSDs shown in Supporting Figures 8S, 9S, and 11S were calculated using a procedure for cylindrical pores and thus underestimated the diameter of cage-like pores.[54] This is clear when the pore cage diameters evaluated from PSDs are compared with those calculated using eq 1 (see Tables 1, 2, and Supporting Table 5S). It is concluded that the PSD calculation method used herein, which was calibrated for cylindrical pores, underestimates the diameter of large cage-like pores by about 2 nm, as expected from earlier studies.[54,71]

Low-Pressure Adsorption on FDU-1 and the Pore Entrance Size Estimation. An experimentally measured adsorption branch of the isotherm for a given sample is a superposition of contributions from adsorption in all kinds of accessible pores present in the sample. Because of that, in principle it should be possible to obtain information about the pore entrance size not only from the desorption branch of the isotherm in the hysteresis region, but also from the adsorption branch. However, it is not easy to explore this opportunity in the case of FDU-1, as this silica features different kinds of pores, including abundant micropores in the pore walls, in addition to the ordered cage-like mesopores and the connecting pores between the cages. Moreover, the pores that connect the mesopore cages may exhibit a shape appreciably different from cylindrical, and thus, their narrowest part (referred to as the pore entrance) may have a diameter appreciably different from the average diameter of

(83) Che, S.; Kamiya, S.; Terasaki, O.; Tatsumi, T. *J. Am. Chem. Soc.* **2001**, *123*, 12 089−12 090.

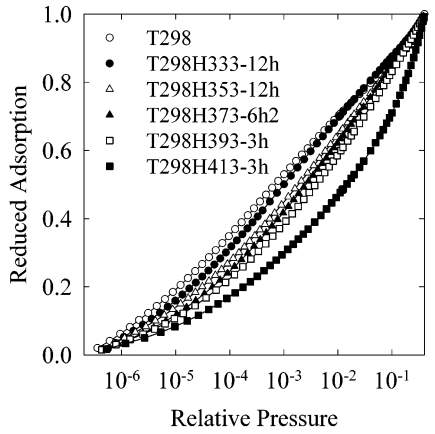

Figure 7. Low-pressure reduced adsorption curves (amounts adsorbed divided by the amount adsorbed at a relative pressure of 0.4) for FDU-1 samples synthesized at room temperature and hydrothermally treated at different temperatures ranging from 333 to 413 K.

the connecting pore. To examine if one can estimate the pore entrance size from adsorption branches of isotherms, nitrogen adsorption data at relative pressures below 0.4, which reflect the micropore filling and capillary condensation in pores of diameter up to about 4 nm,[70,75] were carefully examined. This arbitrarily chosen pressure range is expected to be suitable for FDU-1 silicas, because earlier studies indicated the pore entrance sizes of about 1.3 and 2.4 nm in two typical FDU-1 preparations,[55] and in addition, the existence of pore entrance sizes larger than 4 nm can be inferred from the shape of desorption branches of argon and nitrogen isotherms. To facilitate the comparison, the adsorption data are shown in Figure 7 and Supporting Figure 12S in a logarithmic scale as reduced adsorption curves, that is, as amounts adsorbed divided by the amount adsorbed at a relative pressure of 0.4. The samples synthesized at room temperature and then subjected to further hydrothermal treatments at different temperatures, as well as the samples synthesized in one step at different temperatures were examined. It was found that the reduced adsorption was the highest for the T298 and T303 samples synthesized at room temperature (see Figure 7). As mentioned above, T303 was reported to exhibit an average pore entrance size of about 1.3 nm. The reduced adsorption was systematically decreased as the synthesis temperature was increased, and in particular, it was much lower for the T298H373−6h2 sample that was reported to exhibit an average pore entrance size of about 2.4 nm. The T333 sample was an exception (see Supporting Figure 12S), but it also exhibited exceptionally low pore diameter and adsorption capacity (see Table 1), so it is likely not to be representative and thus can be disregarded. T363 and T298H413−3h samples that featured a fraction of pore openings above 5 nm clearly exhibited the lowest reduced adsorption. Interestingly, several samples were found to exhibit reduced adsorption intermediate between that of the T298/T303 samples and that of the T298H373−6h2 sample. This strongly indicates that for the T298H333−12h, T298H353−12h, and T313 samples that exhibited these intermediate behaviors, the average pore entrance size is between about 1.3 and 2.4 nm. Moreover, the average pore entrance size for the T298H393−3h sample is likely to be slightly above 2.4 nm, as this sample exhibited a reduced adsorption lower than that of the T298H373−6h2 sample. It should be noted that this purely empirical way of obtaining information about pore entrance sizes on the basis of the comparison of reduced adsorption for the FDU-1 samples with those for the FDU-1 silicas of otherwise known pore entrance sizes has its justification in the current knowledge of adsorption behavior in micropores and mesopores. Namely, it is known that the micropore filling or capillary condensation pressure gradually increases as the pore diameter increases (for pores that are wider than the dimensions of adsorbed molecules).[84] Because of that, the micropore filling or capillary condensation takes place at lower pressures in samples with smaller pore entrance sizes, leading to an enhanced reduced adsorption at lower pressures.

4. Conclusions

On the basis of extensive TEM and SAXS characterization, FDU-1 silica was identified as a cubic face-centered structure with intergrowths of 3-D hexagonal structure, thus being similar to SBA-2 and SBA-12 silicas, whose structures were elucidated earlier by using TEM. No evidence of the formation of the *Im*3*m* structure, which was originally reported to be characteristic of FDU-1, was found on the basis of TEM, SAXS, and XRD. FDU-1 silicas with very similar XRD patterns form in a wide range of temperatures, and after formation at a lower temperature, they can be subjected to a hydrothermal treatment at a higher temperature. The increase in temperature typically results in an increase of the unit-cell size, pore diameter and pore entrance size. However, the uniformity of the pore entrance size deteriorates at excessively high temperatures in a one-step procedure or during overly long hydrothermal treatments at sufficiently high temperatures. The most convenient way to tailor the pore size of FDU-1 with good-quality cage-like pore structure is to synthesize this material at room temperature and then subject it to a hydrothermal treatment at judiciously chosen temperature for an appropriate period of time. Ordered materials with uniform pore size and more open pore structures without uniform pore entrance size can be obtained using a one-step synthesis at above 353 K, or a two-step procedure with the second step at or above 373 K.

Acknowledgment. M.J. acknowledges support by NSF Grant CHE-0093707. J.R.M. and L.P.M. acknowledge support by FAPESP, Brazil (Grants 99/11170-5, 99/11171-1). O.T. thanks CREST, JST for financial support, and L.Z. thanks Professor S. Qiu for his encouragement. T.J.P. acknowledges the support of the NSF grant CHE-9903706. The authors thank Dr. Rene Geiger from Dow Chemicals for providing the triblock copolymer.

Supporting Information Available: Figures (17) with TEM images (5), ED patterns (1), positions of peaks on SAXS patterns (1), powder XRD patterns (3), nitrogen adsorption isotherms (1), pore size distributions (4), reduced adsorption curves (1) and α_s plots (1). Tables (5) with indexing of ED patterns (2) and SAXS patterns (2), and with structural properties (1). Supporting discussion of: (i) the structure of T303 FDU-1 sample on the basis of HRTEM and ED, and (ii) prospects of evaluation of pore entrance sizes on the basis of PSDs. This material is available free of charge via the Internet at http://pubs.acs.org.

JA0283347

(84) Cracknell, R. F.; Gubbins, K. E.; Maddox, M.; Nicholson, D. *Acc. Chem. Res.* **1995**, *28*, 281−288.